The effect of spatial luminance distribution on dark adaptation

The effect of spatial luminance distribution on dark adaptation

Mariska G. M. Stokkermans Eindhoven University of Technology, Eindhoven, The Netherlands

Ingrid M. L. C. Vogels Eindhoven University of Technology, Eindhoven, The Netherlands

Ingrid E. J. Heynderickx Eindhoven University of Technology, Eindhoven, The Netherlands

Recent studies show that dark adaptation in the visual system depends on local luminance levels surrounding the viewing direction. These studies, however, do not explain to what extent veiling luminance is responsible for the outcome. To address the latter, in this study dark adaptation was measured for three different spatial luminance distributions surrounding a target to be detected, while keeping the veiling luminance at the location of the target equivalent. The results show that a background with bright areas close to the viewing direction yields longer adaptation times than a background with bright areas at a larger visual angle. Therefore, we conclude that dark adaptation is affected to a great extent by local luminance, even when controlling for veiling luminance. Based on our results, a simple but adequate model is proposed to predict the adaptation luminance threshold for backgrounds having a nonuniform luminance distribution.

Introduction

In order to increase its dynamic range, the visual system adjusts its sensitivity to visual stimuli, a process known as visual adaptation. The type of adaptation addressed in this paper is dark adaptation. It is the process by which the visual system adjusts its sensitivity to dim light after being exposed to bright light, as has been extensively studied in literature (Baker, 1953, 1963; Haig, 1941; Hecht, Haig, & Chase, 1937; Hecht, Haig, & Wald, 1935; Mote & Riopelle, 1951; Ruseckaite, Lamb, Pianta, & Cameron, 2011; Wald & Clark, 1937). Typically, these studies determine the temporal change in the lowest perceptible luminance, known as the luminance threshold or adaptation threshold. This temporal change, in general, is often determined by measuring luminance thresholds at predetermined adaptation times. Participants first preadapt to a bright stimulus and are then asked to detect the target in an otherwise spatially uniform dark background. Several studies have demonstrated that the luminance of the target that can be detected at a given point in time depends on the luminance and duration of the preadaptation stimulus: a higher luminance level or longer duration of the preadaptation stimulus results in a higher luminance threshold (Haig, 1941; Hecht et al., 1937; Mote & Riopelle, 1951; Wald & Clark, 1937). Further, Hecht, Haig, and Wald (1935) investigated the effect of the location of the target with respect to the viewing direction. They showed that the luminance that can be detected after dark adapting for several minutes is lower for a target presented in the periphery (at 5° or 10° visual angle with respect to the viewing direction) compared to a target presented at the fovea (at 0° visual angle). The majority of these past studies have measured the adaptation time up to 30 minutes, but with limited accuracy for the first seconds of dark adaptation. Baker (1953, 1963) used a slightly different methodology and was able to show that the luminance threshold decreases drastically during these first seconds.

The studies mentioned so far have limited value for predicting dark adaptation in daily life circumstances, since they describe dark adaptation to spatially uniform backgrounds, neglecting the spatial complexity of the background, usually occurring in daily life visual stimuli. For example, the field of view of a motorist driving at night exists as a combination of dark areas and very bright spots due to head lights and street lights. In order to predict the visibility of a dim object

Citation: Stokkermans, M. G. M., Vogels, I. M. L. C., & Heynderickx, I. E. J. (2016). The effect of spatial luminance distribution on dark adaptation. *Journal of Vision, 16*(8):11, 1–15, doi:10.1167/16.8.11.

doi: 10.1167/16.8.11 Received October 5, 2015; published June 14, 2016 ISSN 1534-7362

in such circumstances, it is crucial to understand how the visual system adapts to a combination of luminance values in the field of view.

Literature shows that adaptation does not take place globally (i.e., assuming that the entire retina is adapted to the same luminance), but takes place locally (i.e., in smaller parts of the retina) or even at the level of the photoreceptors. For rods, research has shown that, simultaneous excitation of a number of rods is needed for adaptation to occur (Rushton & Westheimer, 1962). For cones, on the other hand, although we are not aware of studies directed at the human eye, studies with primates have shown that each single cone adapts individually to the light levels presented in the receptive field of the cone (Lee, Dacey, Smith, & Pokorny, 1999). Yet for cats, evidence exists that, as cones are connected by horizontal cells, each cone is to some extent also affected by the response of neighboring cones (Lankheet, Przybyszewski, & van de Grind, 1993). Based on these principles, a new local cone model to predict contrast sensitivity in digital imaging has been developed recently, taking into account adaptation to each individual pixel in a displayed image (Daly & Golestaneh, 2015). According to this model the luminance threshold for a nonuniform background is not necessarily equal to the luminance threshold for a uniform background with the same averaged luminance. A recent study of Stokkermans and Heynderickx (2014) showed that the time required to detect a dim target in a dark background containing a bright source increases when decreasing the distance between the source and the target. This suggests that dark adaptation strongly depends on local luminance levels surrounding the target to be detected. Additionally, Uchida and Ohno (2013) studied dark adaptation for a peripheral task. In this study, participants had to look at the center of a display, but were asked to detect a target presented at a distance of 10° from the center. The background of the target had either a spatially uniform luminance, or contained a circular pattern of 12.4° around the target while the rest of the background was dark. The luminance threshold for the nonuniform background was higher than for the uniform background, although the average luminance was equal for both backgrounds. However, when the luminance of the circular pattern equaled that of the uniform background so that the average luminance of the nonuniform background was lower than that of the uniform background, both luminance thresholds were equal. Therefore, Uchida and Ohno (2013) concluded that the luminance threshold mainly depends on the local luminance surrounding the task area.

A factor not explicitly controlled in these studies is veiling luminance, which is the luminance superimposed over the retinal image, caused by stray light within the eye. So, a bright source in a dark background can cast a "veil" over the field of view, which leads to a reduction in contrast between target and background, and subsequently to a reduction in visibility (Holladay, 1926). Veiling luminance can be roughly described by a $1/\theta^2$ function, where θ indicates the visual angle between the source and the viewing direction, in degrees. Hence, it increases with decreasing visual angle. Thus, when a bright source is close to a target, the source may reduce the target's visibility, and as such influence the luminance threshold. Uchida and Ohno (2013) evaluated the possible impact of veiling luminance on the luminance threshold of a peripheral target detection (as described above) by comparing two types of models: the first type only accounted for the local background luminance surrounding the task (i.e., the luminance in the 12.4° circular pattern), whereas the second type also accounted for veiling luminance. Based on their results they concluded that the luminance threshold mainly depends on the local background luminance values and that veiling luminance plays a minor role. Nevertheless, they suggest that veiling luminance may have a larger influence on the luminance threshold of targets for a background at relatively high luminance. Contrary to the main finding of Uchida and Ohno (2013), Langendijk and Hammer (2010) found that veiling glare heavily reduced perceived contrast, in a study investigating the maximal spatial luminance variation distinguishable in high-contrast images displayed on an LCD display. In their study, the potential effect of adaptation was not taken into account as it was said to have a much smaller effect than veiling glare.

Several models have been proposed to describe the combination of luminance adaptation and veiling luminance. Murdoch and Heynderickx (2012) studied the visibility of black level differences between two nonuniform images in the proximity of a bright source. In their model, veiling luminance was described by the CIE general glare equation based on the report of Vos and van den Berg (1999). This equation depends, aside from the visual angle to the bright source, on the pigmentation level of the eye and the age of the observer. Luminance adaptation was calculated by weighting the luminance of each pixel by two Gaussians: a first narrow Gaussian ($SD = 0.67°$) with a high weight, representing the foveal contribution, and a second broader Gaussian ($SD = 3.9°$) with a lower weight, representing the peripheral contribution. Focusing on the central part of the fovea only, Vangorp, Myszkowski, Graf, and Mantiuk (2015) created a model of local adaptation, using a similar approach as Murdoch and Heynderickx (2012). In their best performing model, veiling luminance was modelled using the optical transfer function of Deeley, Drasdo, and Charman (1991) and luminance adaptation by two Gaussians with standard deviations of 0.428° and

0.082°. Also Normann, Baxter, Ravindra, and Anderton (1983) modeled the input stage of the eye. This model focused on cone vision only, and assumed local adaptation of each cone. On top of this, they used a point spread function combined of several functions modeling veiling luminance for various visual angles, and a function accounting for involuntary eye movements up to 1°, basically spreading out the retinal image to some degree.

Existing literature suggests that target detection during dark adaptation may be affected by a combination of local luminance and veiling luminance. However, to the best of our knowledge there is no empirical study neatly controlling for the effect of veiling luminance while investigating dark adaptation. Therefore, the main objective of the present study is to investigate the effect of different spatial luminance distributions in the background on dark adaptation, while keeping the veiling luminance on the target area equivalent.

The remainder of this paper first describes the empirical experiment investigating the effect of the spatial luminance distribution of the background on the adaptation time required to detect targets of different luminance. In contrast to many previous studies, the target luminance was varied and the adaptation time was the dependent measure. This allowed us to vary the location of the target, to verify if the target was actually detected, and thereby control for potential incorrect answers. The experimental results are then modeled with a combination of local background luminance and veiling luminance, resulting in a prediction of the luminance threshold as a function of time for backgrounds having a nonuniform luminance distribution.

Method

In order to study the effect of spatial luminance distribution of the background on the adaptation time, two experiments were conducted. In Experiment E1, already discussed in Stokkermans and Heynderickx (2014), the adaptation time was measured for several target luminance levels presented on a spatially uniform dark background, whereas in Experiment E2, the adaptation time was measured for more target luminance levels on spatially nonuniform backgrounds. Both experiments consisted of two tasks: a reaction time task and an adaptation task. In the reaction time task, the measured reaction time consisted of the time needed to detect the target and to respond to the target. In the adaptation task, the measured adaptation time included the time needed to adapt to the lower luminance level, to detect the target, and to respond to the target. Our main goal was to measure only the time needed to adapt to the change in luminance level. Therefore, each participant's reaction time was subtracted from the adaptation time, resulting in a measure of dark adaptation time exclusively, called the net adaptation time. A follow-up of Experiment E2 was also conducted, monitoring eye movements during the adaptation task.

Experimental set-up

All experiments were conducted in one of the labs of Philips Research in Eindhoven. As described in full detail in Stokkermans and Heynderickx (2014), a black viewing box was placed on a table in front of a monitor (FIMI-Philips 18-in. SXGA, 1280 × 1024 pixels). The monitor was a monochrome medical display, with two liquid crystal layers in front of a fluorescent backlight. The spatial luminance uniformity of the display was measured using a Radiant Imaging ProMetric luminance camera (Radiant Image Systems, Redmond, WA). The luminance of the displayed image was adapted to correct for spatial luminance deviations of the display. After correction, the monitor reached a maximum luminance of 650 cd/m^2 and a minimum luminance of 0.0065 cd/m^2. The viewing box consisted of a cutout through which the center of the monitor was visible. The viewing distance of the participant was fixed by means of a chinrest and corresponded to 0.75 m from the monitor. This resulted in 46.7 pixels/° of visual angle, and a visible area of the monitor of 20° × 20°.

Eye tracking measurements were conducted using a SMI RED system (SensoMotoric Instruments, Teltow, Germany). The SMI RED device provided information on the position of the left and the right eye individually, with a time interval of 8 ms.

Stimuli

The preadaptation stimulus consisted of a white image of 20° × 20° with a luminance of 650 cd/m^2. The adaptation stimuli consisted of a black image of 20° × 20° with a luminance of 0.0065 cd/m^2 and with a target superimposed on it. The target was located at 4.3° visual angle left or right from the center of the image. It was shaped like a circle of equal luminance, with a diameter of 0.43° and with an edge of decreasing luminance. The target was created with a Gaussian filter ($\sigma = 0.21°$), topped off at half its height. Figure 1 depicts a cross section of the target. The luminance levels used for the target during the adaptation task of Experiment E1 and Experiment E2 are presented in Table 1 (and refer to the luminance of the center 0.43°

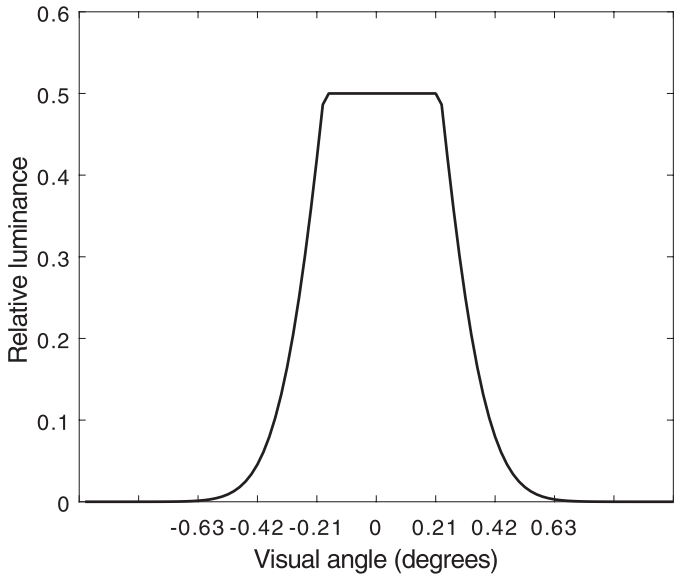

Figure 1. Cross-section of the target. On the *x*-axis the visual angle in degrees is shown, and on the *y*-axis, the relative luminance is shown.

of the target). All luminance levels were measured using a PhotoResearch SpectraDuo PR 680 luminance camera (PhotoResearch, Chatsworth, CA), set to an aperture size of 1/8°. During the reaction time task, a stimulus with a target luminance level of 277 cd/m^2 was used. Obviously, this target luminance was high, so the target was immediately visible to all participants.

For Experiment E1, the black (background) image (as depicted at the top left of Figure 2) was basically spatially uniform, although it did contain a small plus symbol with a size of 0.47° by 0.47° and a luminance of 10 cd/m^2. The plus symbol was centered horizontally, at 10° visual angle from the target. The reason for the addition of this plus symbol was, as discussed in full detail in Stokkermans and Heynderickx (2014), to provide the participants with an orientation point towards the possible position of the target. This orientation marker allowed for a better comparison of the uniform background to the spatially nonuniform backgrounds, as the latter inherently also contained cues on the possible location of the target. The background used in Experiment E1 is further referred to as *Uniform*. For Experiment E2, the black background image was replaced by three images with a different luminance distribution, as also depicted in Figure 2. Further, Table 2 presents an overview of all background variations of Experiments E1 and E2.

The background images for Experiment E2 were created such that the luminance distribution differed, but the veiling luminance at the center of the target was equivalent and the average luminance of the entire image was equal for two of the three images (since it was intrinsically impossible to do it for all three

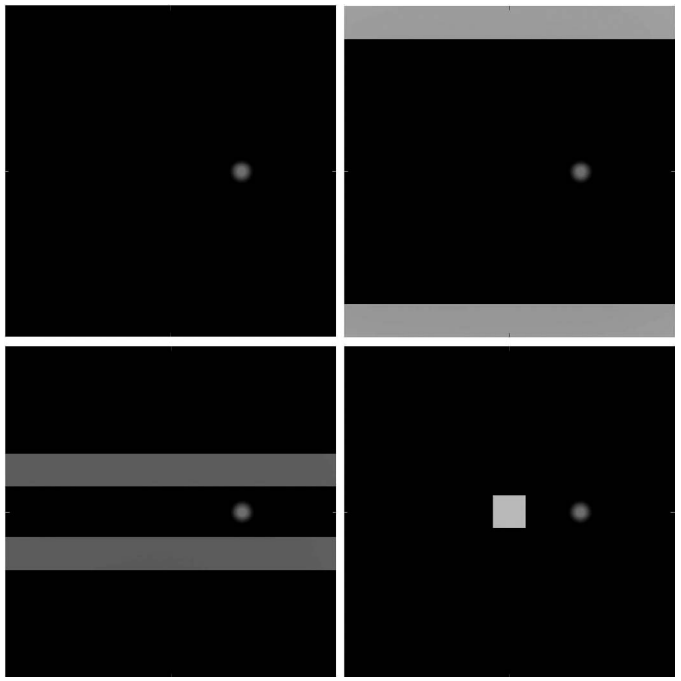

Figure 2. Luminance distribution of the four background images used in Experiments E1 and E2. The top left image shows the *Uniform* background. The top right image shows a background containing two bars at 9° from the target (i.e., *Bar9*). The bottom left image shows a background with two bars at 2.7° from the target (i.e., *Bar2.7*). The bottom right image shows a background with a squared area in the center of the image, at 4.3° from the target (i.e., *Square*). In all backgrounds, the target may appear on the right side of the center (as depicted), as well as on the left side of the center.

images). The first background image (shown at the top right of Figure 2, and referred to as *Bar9*) had 2 horizontal bars with a width of 2° at a 9° distance from the target. The luminance of the bars was 42 cd/m^2. The second background image (shown in the bottom left of Figure 2, and referred to as *Bar2.7*) contained two horizontal bars with a width of 2° at a 2.7° distance

Luminance of the target (cd/m^2)	
Experiment E1	Experiment E2
11.19	11.19
0.223	–
0.056	0.056
–	0.045
0.036	0.036
–	0.028
0.023	0.023
–	0.018
0.014	0.014

Table 1. Overview of target luminance levels, for Experiments E1 and E2.

Experiment	Luminance distribution	Average luminance (cd/m^2)	Veiling luminance (cd/m^2)
E1	*Uniform*	0.0065	–
E2 (and eye-tracking experiment)	*Bar9*	8.41	0.07
	Bar2.7	1.02	0.07
	Square	1.02	0.07

Table 2. Overview of background luminance distributions for Experiments E1 and E2.

from the target. The luminance of these bars was 5.1 cd/m^2. The third background image (shown at the bottom right of Figure 2, and referred to as *Square*) contained a squared area of 2° by 2° in the center at a 4.3° distance from the target. The luminance of this squared area was 101 cd/m^2. The luminance averaged over the entire image was 1.02 cd/m^2 for *Bar2.7* and *Square,* and 8.41 cd/m^2 for *Bar9,* as indicated in Table 2. The veiling luminance at the center of the target, calculated with the general glare equation defined by Vos and van den Berg (1999), was 0.07 cd/m^2 for all three backgrounds. All values of location and luminance of the bars and square were chosen based on two grounds, also using a pilot experiment: (a) the veiling luminance at the location of the target had to be equal for all backgrounds, and (b) most targets had to be detected within 60 s, as this time limit was also used in Stokkermans and Heynderickx (2014). The task of the participants was equal to the adaptation task of Experiments E1 and E2, as described later in this Method section. After being exposed to the preadaptation stimulus, the participants were asked to detect a target in the various image backgrounds. The time it took to adapt to the luminance of the target was measured.

Experimental design

In Experiment E1, a full-factorial within-subject design was used with one independent variable (i.e., the luminance of the target). Experiment E2 used a mixed within-subject and between-subjects design with two independent variables, namely the luminance of the target and the background. Since the number of stimuli was substantially larger in Experiment E2, a D-optimal design was used to compute the most optimal design, given the number of participants and variables (Eriksson, 2008), which resulted in a selective number of target luminance levels per background for each participant. Both independent variables were proportionally distributed over all participants, and in total presented an equal number of times.

Participants

Six participants (four men and two women) joined Experiment E1. Their average age was 28 years with a standard deviation of 5.1 years. In total, 30 participants (19 men and 11 women) joined Experiment E2. They had an average age of 28 years with a standard deviation of 7.3 years. Five participants (four men and one woman) were asked to take part in the eye tracking experiment. Their average age was 26 years with a standard deviation of 2.7 years. This study was approved by the review board of the Eindhoven University of Technology, adhering to the Code of Ethics of the Dutch Institute for Psychologists, as well as by the ethical committee of Philips Research, adhering to the Declaration of Helsinki.

Procedure

Figure 3 presents a schematic overview of the chronologic procedure in both experiments. First, in both experiments, participants were invited into our laboratory, signed the informed consent form, and were given instructions on the experiment. After that, the participants sat down in front of the monitor and conducted a short practice run in order to get familiar with the procedure. Then, the ambient light in the room was turned off, and participants started with the reaction time task. They were asked to look at the

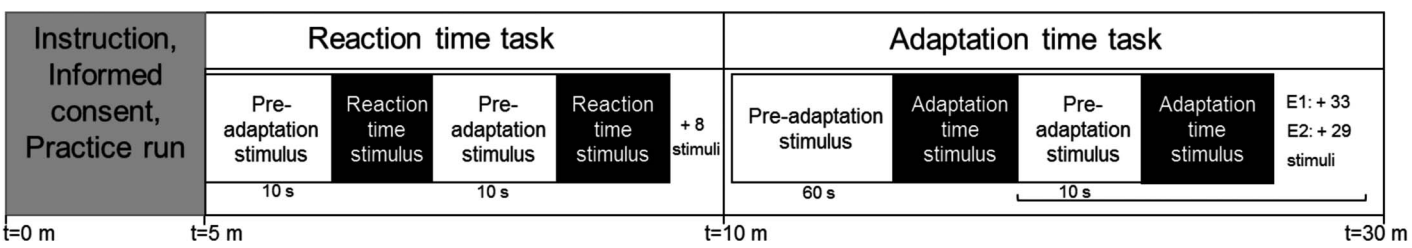

Figure 3. Schematic overview of chronologic procedure of Experiments E1 and E2.

preadaptation stimulus for 10 s, after which an image with an easily detectable target on a background was presented. The backgrounds used were *Uniform* for Experiment E1 and *Bar9* for Experiment E2. Participants had to indicate as quickly as possible whether the target was presented at the left or the right side of the center of the image, using the arrow keys of a keyboard. They were asked to be both accurate and quick in detecting and reporting the target. This task was repeated 10 times with the target presented randomly at the left or the right side.

After the reaction time task was finished, the participants continued with the adaptation task. In this case, they first had to adapt to the preadaptation stimulus for 1 min preadaptation time. This time period of light adaptation was implemented so that every participant (irrespective of previously experienced light conditions) would start at the same adaptive state. Then, the adaptation stimulus was shown and the eye started to adapt to the lower luminance level. It was the task of the participants to report the location of the target, either left or right from the center of the image, using the arrow keys of a keyboard. The time they needed to be adapted enough to detect and report the target is referred to as adaptation time. Again, participants were asked to be both accurate and quick in detecting and reporting the target. Between two successive adaptation tasks, the preadaptation stimulus was shown again for 10 s, considered to be sufficient since adaptation to light stimuli proceeds much faster than to dark stimuli (Crawford, 1947; Hood & Finkelstein, 1986). In Experiment E1, each target luminance was assessed six times by all participants only for the background *Uniform*. In Experiment E2, all participants assessed one to four target luminance levels for every background (i.e., *Bar9, Bar2.7, and Square*), with four repetitions. In both experiments, all stimuli were presented in a random order to each participant. Note that the adaptation time per stimulus was limited to 1 min because of our main interest in early adaptation. Once the participants completed the experiment, they were debriefed and thanked for their participation.

To gain more insight in the participants' course of actions to detect the target, a follow-up experiment, monitoring eye movements during the adaptation task, was conducted. This follow-up experiment used a subset of the stimuli of Experiment E2, namely only three target luminance levels for each of the three backgrounds. Since the use of the eye tracker demanded more light, ambient illumination (185 lux on the desk) was provided in the lab and the viewing box was removed. Obviously, the measured adaptation times during this follow-up experiment were not used for further analysis.

Analyses

For the reaction time task, incorrect responses (i.e., indicating the target to be left when it actually was right, or vice versa) were removed. The remaining observations within each participant were then checked for outliers, using the criterion of more than 3 standard deviations away from the average (Osborne & Overbay, 2004). As this wasn't the case for any of the observations, no additional measurements were removed. The intrinsic reaction time for every participant was calculated as the average of the remaining measurements.

The data for the adaptation task were treated in a similar way. First, incorrect answers were removed. However, in order to prevent the chance of guessing becoming too high, if more than one incorrect answer was given for a certain stimulus, all measurements of the corresponding stimulus were removed for that participant. Further, when the time limit of 60 s was reached, the measurement was set to an adaptation time of 60 s. Lastly, we analyzed if any of the participants could be identified as outlier, again using the criterion of 3 standard deviations away from the averaged performance. As this wasn't the case for any of the participants, no outliers were removed.

The net adaptation time was then determined by subtracting the intrinsic reaction time from the measured adaptation time. The net-adaptation time data were analyzed with two linear mixed models (LMM) using SPSS IBM Statistics 20. An LMM is a mean comparison statistical analysis, comparable to an analysis of variance (ANOVA). In contrast to least square fitting used by an ANOVA, an LMM uses maximum likelihood. Compared to ANOVAs, LMMs are therefore more robust to balanced incomplete designs, as is used in Experiment E2. The independent variables were target luminance and luminance distribution of the background. The first LMM analysis analyzed the data of Experiment E2. Target luminance consisted of the eight levels specified in Table 1. Luminance distribution consisted of three levels, namely: *Bar9, Bar2.7,* and *Square*. The second LMM compared the net adaptation time of the uniform background to the nonuniform backgrounds, and hence, contained the data of Experiments E1 and E2. Target luminance now consisted of the five luminance levels that were tested in both experiments (i.e., 11.17 cd/m^2, 0.056 cd/m^2, 0.036 cd/m^2, 0.023 cd/m^2, 0.014 cd/m^2). Luminance distribution existed of four levels, namely: *Uniform, Bar9, Bar2.7,* and *Square*. The effect of participant was modeled as a random intercept. This accounts for a general offset in the adaptation time between participants; for example, some participants may intrinsically adapt slower than others (similarly for all target luminance values). Further, the interaction of target luminance level and participants was modeled (as

a random slope). This allowed the LMM to account for variations in the slope of the participants' luminance thresholds as a function of time. In both LMM analyses, a Bonferroni correction was used to analyze the pairwise comparison effects within and between the two independent variables. The dependent variable of both LMMs was the ^{10}log net adaptation time, as the data were more normally distributed in the ^{10}log space.

Eye-tracking measurements

Points-of-regard were analyzed in terms of the spatial x and y dimensions of the background. First, the raw data were corrected for a systematic offset of approximately 70 pixels (1.5°) in the y dimension. Then, all data where the target was presented on the left side of the background were mirrored with respect to the horizontal center of the image in order to combine them with the data for which the target was presented on the right side of the background. Last, the data of the left eye and the right eye were averaged. Based on these data, two different types of graphs were created. The first type depicted the spatial distribution of the points-of-regard per background combining all participants. The second type depicted the trajectory of the point-of-regard over time per participant.

Results

Reaction time task

In the reaction time task of Experiment E1 (using the background *Uniform*), two incorrect (3.3%) answers in total were given, and seven incorrect answers (2.3%) were given in the reaction time task of Experiment E2 (using background *Bar9*), indicating that the participants in general were very accurate in their response. After removing these incorrect responses, the average reaction time for experiment E1 became 0.55 s with a standard deviation of 0.15 s, and for Experiment E2, 0.44 s with a standard deviation of 0.12 s. An independent samples t test showed that these reaction times were significantly different, $t(349) = 4.88$, $p < 0.001$. Since the target was easily visible on both backgrounds used (*Uniform* for E1 and *Bar9* for E2), we did not expect a significant difference between the two backgrounds. It might be that the additional bars in the background of *Bar9* directed the participants to the expected target location, and as such facilitated the task. The difference in reaction time could also be attributed to the different participants used.

Adaptation task

For the adaptation task of Experiment E1, only one incorrect answer (0.4%) was removed, while seven incorrect answers (0.7%) were removed for the adaptation task of Experiment E2. Additionally, in Experiment E2, one participant incorrectly indicated the location for the same target and background twice. Therefore, all four data points for that target and background combination were removed from further analyses. Again, the limited number of incorrect responses shows that the participants were quite accurate in their responses.

For Experiment E1, no measurements exceeded the 60 s limit, while for Experiment E2, this happened in total 66 times (i.e., 6.9%). This occurred mostly (i.e., 44 times) for backgrounds *Bar2.7* and *Square* when detecting the target with the lowest luminance of 0.014 cd/m^2. For these latter two stimuli, data with an adaptation time longer than 60 s accounted for 55% of the measurements. Setting the adaptation time to 60 s led to a somewhat skewed distribution for this level.

Statistical analyses

Figure 4 graphically depicts the means and 95% confidence intervals, calculated with the raw data (excluding incorrect responses and within the 60 s limit), of the net adaptation time as a function of target luminance level, for all backgrounds. The first LMM, analyzing the data of Experiment E2, revealed a significant effect of target luminance level, $F(7, 180) = 409.0$, $p < 0.001$. In general, the net adaptation time increased with decreasing target luminance. We also found a significant effect of the luminance distribution of the background, $F(2, 274) = 9.4$, $p < 0.001$, on the net adaptation time. Pairwise comparisons revealed that the background *Bar9* led to a significantly shorter adaptation time than the backgrounds *Square* ($p < 0.001$) and *Bar2.7* ($p = 0.039$), while the net adaptation times for the latter two backgrounds were not statistically significantly different from each other ($p = 0.215$). No significant interaction effect between target luminance and luminance distribution of the background was found, $F(14, 287) = 1.6$, $p = 0.073$, but there was a trend showing that the difference in adaptation time between the various backgrounds was larger for lower target luminance levels.

As explained before, for backgrounds *Bar2.7* and *Square* the distribution in net adaptation time was skewed toward 60 s for the lowest target luminance. Therefore, we ran an additional LMM analysis, including only these two backgrounds and excluding the target with a luminance of 0.014 cd/m^2. The results showed a trend toward a longer net adaptation time for the background *Square* than for the background *Bar2.7*, $F(1, 123) = 3.0$, $p = 0.085$. In addition, we found a trend for the interaction between luminance distribution and target luminance, $F(6, 131) = 1.8$, $p = 0.096$, indicating that the difference in adaptation time became larger (with longer

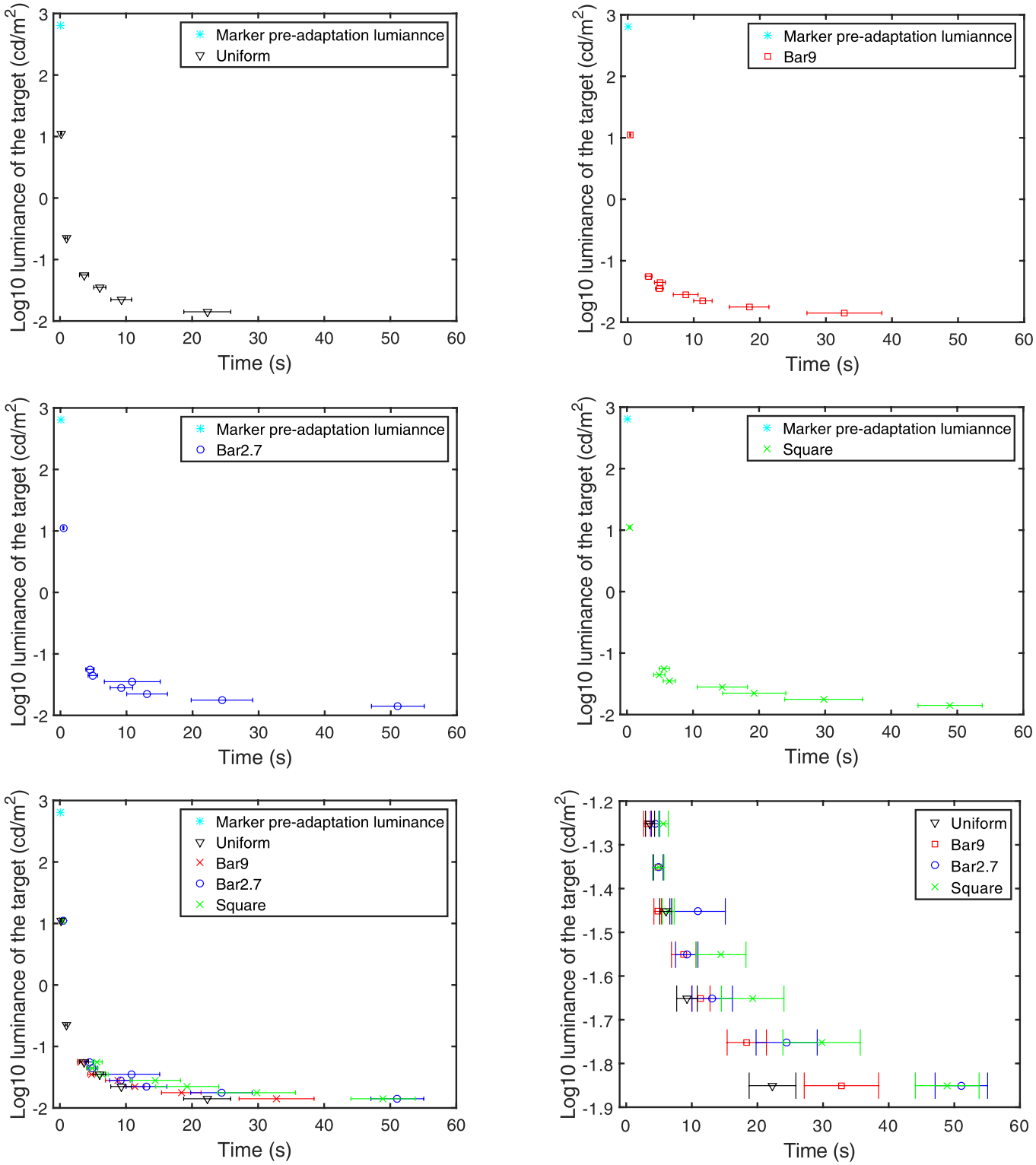

Figure 4. Graphs showing ^{10}log adaptation luminance (in cd/m^2) on the *y*-axis as a function of adaptation time (in seconds) on the *x*-axis for four different backgrounds of the target, namely *Uniform*, *Bar9*, *Bar2.7*, and *Square*. The top four graphs present the results for each of the backgrounds separately. The bottom left graph presents all measured data, and for clarity of interpreting the results, the bottom right graph zooms in on the lowest target luminance levels. The error bars represent 95% confidence intervals.

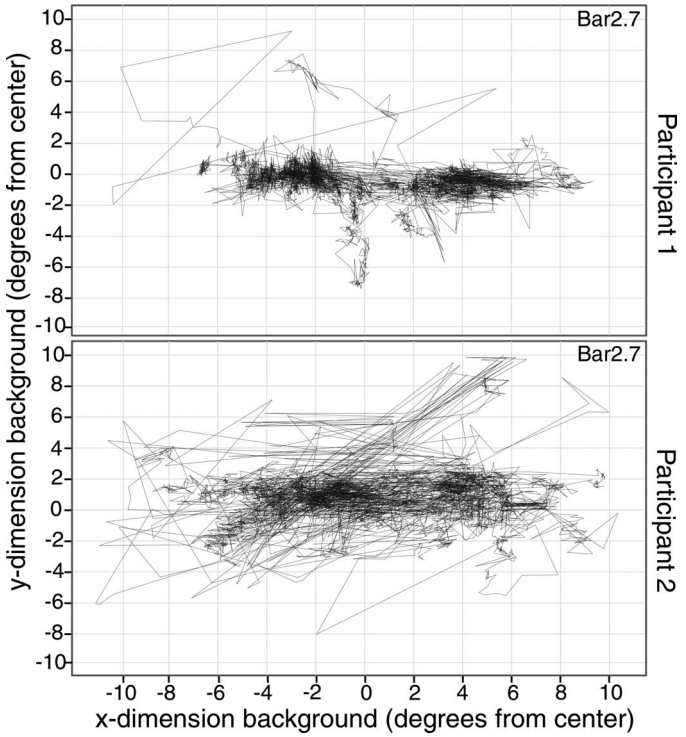

Figure 5. Trajectory of the point-of-regard over time for detecting a target on the *Bar2.7* background for two participants, where the *x*-axis presents the *x*-dimension of the background (in degrees) and the *y*-axis represents the *y*-dimension of the background (in degrees).

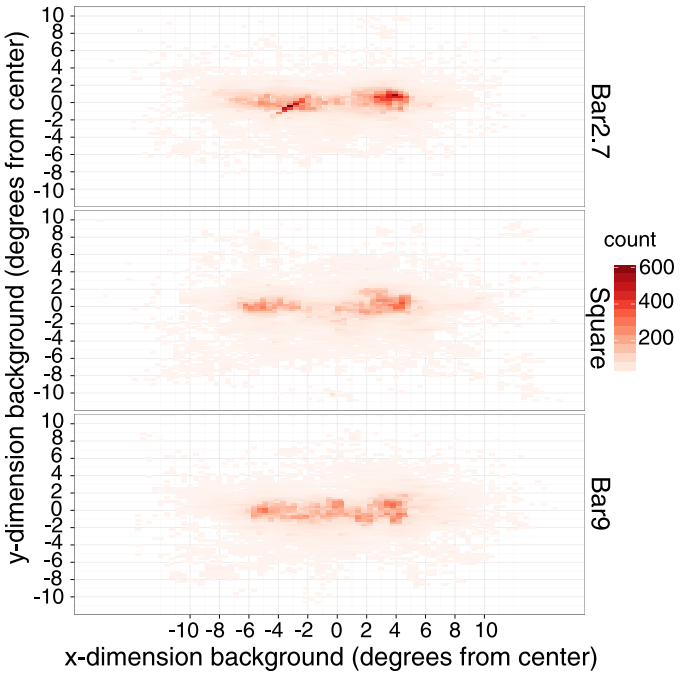

Figure 6. Spatial distribution of the points-of-regard combined for all participants per background.

adaptation times for the background *Square*) for lower target luminance levels. Also in this analysis, the net adaptation time was significantly affected by the target luminance, $F(6, 103) = 186.7$, $p < 0.001$.

The LMM analyzing the data of Experiments E1 and E2, showed a significant effect of target luminance, $F(4, 145) = 505.0$, $p < 0.001$, and luminance distribution of the background, $F(3, 76) = 14.7$, $p < 0.001$, on the net adaptation time. The spatially uniform background resulted in a significantly shorter adaptation time compared to the nonuniform backgrounds, *Square* and *Bar2.7* ($p < 0.001$), and *Bar9* ($p = 0.001$). A significant interaction effect was found between target luminance and the luminance distribution of the background, $F(12, 197) = 10.1$, $p < 0.001$. This interaction effect showed that the difference in adaptation time between the various backgrounds was larger for lower target luminance levels.

Eye-tracking measurements

Visual inspection of the eye tracking measurement data showed that the participants used a similar strategy to locate the target, irrespective of the type of background. Figure 5 depicts, as an example, the trajectory of the point-of-regard over time for two participants, detecting a target on the *Bar2.7* background; these participants basically scanned along the horizontal midline of the background in order to locate the target. Participant 2 occasionally attended the rest of the background more often than participant 1, but most of the points-of-regard were clearly along the horizontal midline.

Figure 6 shows the two-dimensional spatial distribution of all points-of-regard combined for all participants, per background. It clearly illustrates a large concentration of visual attention within the region of the potential target. Participants looked at other parts of the background only sparsely. This tendency was independent of the background for which the target had to be located. The most pronounced difference between the three backgrounds was that for background *Bar9* participants paid slightly more attention to the center of the background than for the backgrounds *Bar2.7* and *Square*.

Interpreting both types of graphs, we find that generally the participants' strategy to locate the target was very similar for all three backgrounds, where they mainly scanned along the horizontal midline, with only sparsely looking at other parts of the background.

Discussion

The objective of this study was to gain more insight into dark adaptation to an environment with

a nonuniform luminance distribution. The main question was whether the visual system adapts to local or global luminance, when corrected for veiling luminance at the center of the target. The results showed that nonuniform backgrounds with a different spatial luminance distribution but with equivalent veiling luminance can lead to different adaptation times. A background having a square in the center and a background with bars close to the target both result in a longer adaptation time than a background with bars at a larger distance from the target. This shows that dark adaptation is to a large extent influenced by the local luminance surrounding the viewing direction, at least for the luminance levels used in our study. This suggests that the visual system adapts at any retinal position to a weighted average of the surrounding luminance. This finding agrees with literature. Uchida and Ohno (2013) found that the visual system locally adapts to the task area, in their case for a peripheral detection task. Further, models using local adaptation such as described by Normann et al. (1983) and Vangorp et al. (2015) were found to accurately predict contrast thresholds for nonuniform images.

Our study shows a trend that the adaptation time is longer for detecting a target in a background having a square in the center (at 4.3° distance) than in a background having two bars at close distance (2°). This may be caused by a difference in the shape of the spatial luminance distribution in relation to the potential location of the target. A different luminance distribution in the local field of view may, as discussed before, lead to a different adaptation time. The eye-tracking measurements showed that the participants scanned along the horizontal midline of the background in order to localize the target. For the background containing the square in the center, such scanning will cause a temporal variation in adaptation luminance, since the visual system adapts to a high luminance while the eyes scan across the square, and to a lower luminance when the eyes look at the possible position of the target. So, since dark adaptation is relatively slow, the visual system at the target detection area may be adapted to a somewhat higher luminance for the background containing the square compared to the background with the bars. This may therefore affect the adaptation time, especially for lower target luminance levels. Nevertheless, as the difference between background *Square* and background *Bar2.7* was not significant, for the target luminance levels assessed in the present study, the effect of scanning over a bright area seems to be of less importance to the adaptation time than the effect of the spatial luminance distribution of the background. To draw a solid conclusion on the effect of temporal variations in local retinal luminance on the adaptation time, more research is required.

Finally, the present study shows that the adaptation time for the spatially uniform dark background is shorter than for all nonuniform backgrounds. Therefore, we may conclude that also luminance in the near periphery of the retina (as is the case for background *Bar9*), affects the adaptation time. The eye-tracking measurements indeed showed that participants did not look at the bright bars in the background, but mainly looked at the middle line. Even though the eye-tracking measurements were taken in a lighted space, literature shows no systematic deviations in eye movements in a dark or in a lighted space for humans (Goffart, Quinet, Chavane, & Masson, 2006; Snodderly, 1987). However, as bright objects are known to attract attention (Vos, 2003), participants may have looked more often to the relatively brighter areas of the background in the actual experiment (since it was executed in the dark space), than recorded by the eye-tracking measurements (executed in the lighted space). Also, veiling luminance could have influenced the adaptation time, since the veiling luminance on the target was smaller for the uniform dark background compared to the nonuniform backgrounds. Finally, neural processes of the visual system may also explain our findings. As described in the Introduction, the first stage of visual processing can be described by a model of local adaptation in combination with factors addressing glare and/or eye movements (Normann et al., 1983). Visual pathways (i.e., magnocellular and parvocellular) from the retina to the lateral geniculate nucleus (LGN) alter the visual signals to some extent. Research has demonstrated that the magnocellular pathway shows local adaptation, whereas little evidence is found for local adaptation of the parvocellular pathway (Pokorny & Smith, 1997). It is possible this might, to a certain extent, explain why luminance at 9° distance affected the adaptation time slightly.

It was the aim of the present study to use an equivalent level of veiling luminance at the target location for all backgrounds. The veiling luminance exceeded the luminance of most of the targets. Thus, its impact is not negligible. Nevertheless, it is unknown to what extent we can extrapolate our findings to apply to conditions with higher veiling luminance levels. Higher levels of veiling luminance, assuming full adaptation, increase the luminance thresholds (Murdoch & Heynderickx, 2012). However, it is unknown if and how higher levels of veiling luminance affect the adaptation threshold as a function of time. Additional research is therefore needed, including various levels of veiling luminance in combination with various background luminance distributions.

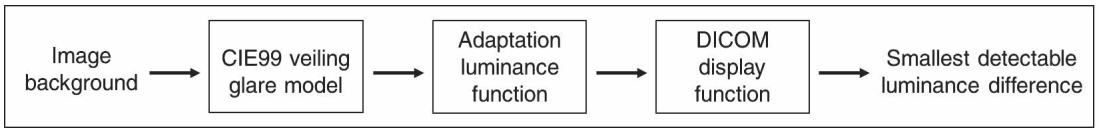

Figure 7. Diagram of black level visibility model used by Murdoch and Heynderickx (2012).

Modeling

In order to generalize our findings, a model is proposed to predict the luminance threshold as a function of time for a nonuniform background. The relatively simple model consists of the black level visibility model of Murdoch and Heynderickx (2012) in combination with the luminance threshold as a function of time for a spatially uniform background. Several other models exist (Normann et al., 1983; Vangorp et al., 2015). These models also combine local adaptation with veiling glare. However, they mainly focus on the region of the fovea and cone vision. In our study both foveal and peripheral vision are important and both rods and cone are involved. Moon and Spencer (1945) considered a foveal size of 1.5°, explaining 92% of the total adaptation, and a surrounding area accounting for effects of veiling luminance, explaining 8%. Hence, this model is conceptually similar, but the sizes are slightly different than used by Murdoch and Heynderickx (2012).

The black level visibility model of Murdoch and Heynderickx (2012) predicts the just noticeable difference in black level—assuming full adaptation—between two nonuniform images in the presence of a glare source. This model consists of three components: the CIE99 glare model, a luminance adaptation function, and the DICOM model. A diagram of the model is depicted in Figure 7.

First, Vos and van den Berg's (1999) CIE135/1 glare model (general glare equation) is used to determine the effect of veiling luminance on the image. As described in the Introduction, this model is based on measurements of the optical performance of the human eye from 0.1° to 100°, which can be roughly described by a $1/\theta^2$ function, where θ indicates the visual angle between the light source and the viewing direction, in degrees. In addition, it accounts for effects of age and eye pigmentation. Next, the luminance of the image in combination with the effect of veiling luminance is used as input for the luminance adaptation function. This function accounts for the fact that the adaptation of the visual system does not take place globally, but locally to a large extent. The function consists of a combination of two Gaussians (depicted in Figure 8), where the first Gaussian function is narrow ($SD = 0.67°$) with a high weight (0.9935) corresponding conceptually to foveal sensitivity, and the second Gaussian function is wide ($SD = 3.9°$) with a low weight (0.0065) corresponding to peripheral sensitivity. The combination of these Gaussians is assumed to be centered on the position of the target. The luminance adaptation function then weights the luminance of every pixel of the image (corrected for veiling luminance) surrounding the target, and integrates the outcome over the whole image. The resulting adaptation luminance is subsequently used as input into the DICOM standard display function (2011), which yields a prediction of the smallest detectable luminance difference. As Murdoch and Heynderickx (2012) stated, the DICOM function was originally developed for a very specific imaging target, however it may be used with caution in other circumstances. A new display function, aimed at high dynamic range displays up to 10000 cd/m^2 has been developed recently (Miller, Nezamabadi, & Daly, 2012). As this extended luminance range was not required for our study, we make use of the DICOM function, to not alter the components as used by Murdoch and Heynderickx (2012). In future studies, it will be interesting to compare these outcomes to the new SMPTE 2084 function.

In order to apply the model of Murdoch and Heynderickx (2012) to predict the luminance threshold for a nonuniform background at several time intervals

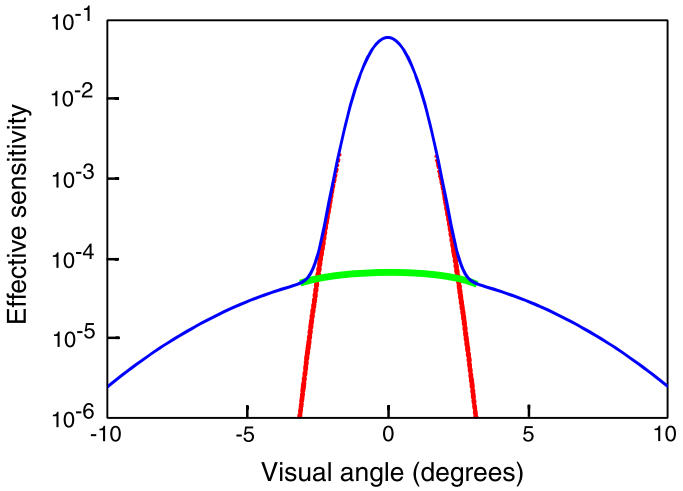

Figure 8. Adaptation luminance curve. The red curve depicts the Gaussian corresponding to foveal sensitivity. The green curve depicts the Gaussian corresponding to peripheral sensitivity. The blue curve shows the combined sensitivity of the two Gaussians. This figure is slightly adapted from Figure 10 depicted in Murdoch and Heynderickx (2012), with permission of the publisher.

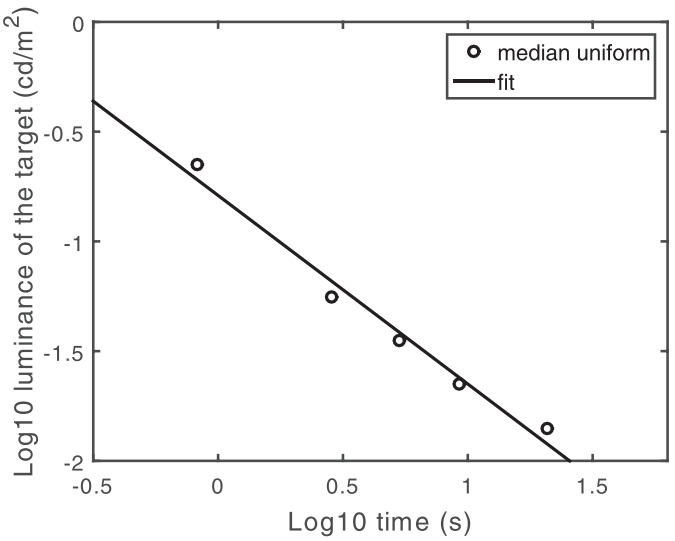

Figure 9. The ^{10}log luminance of the target (in cd/m^2, presented on the *y*-axis) as a function of the ^{10}log adaptation time (in seconds, presented on the *x*-axis) for the spatially uniform dark background used in Experiment E1. The solid line shows the fitted linear relation $y = a \times x + b$, with *y* the ^{10}log luminance (in cd/m^2) and *x* the ^{10}log time (in seconds). The fitting parameters are: $a = -0.86$ with a 95% confidence interval of $(-1.08, -0.63)$, and $b = -0.79$ with a 95% confidence interval of $(-0.98, -0.60)$.

during dark adaptation, it should be extended with a function describing the luminance threshold as a function of time for a spatially uniform background. This function is known from literature, albeit not very accurately in the first seconds. Therefore, our data of Experiment E1 was used to deduce the luminance threshold as a function of time, by fitting the linear relation $y = a \times x + b$, with y the ^{10}log luminance (in cd/m^2) and x the ^{10}log time (in seconds), using the least squares approach. The result is plotted in Figure 9. The adjusted R^2 was 0.97. The target with a luminance of 11.19 cd/m^2 was excluded from this fit, since it was detected almost instantaneously. Therefore, we expect that no adaptation was required to detect that target.

Combining the black level visibility model with the luminance threshold as a function of time for a spatially uniform dark background, leads to the model as presented in Equation 1:

$$L_{nu}(t) = L_u(t) + DICOM\Big(ALF\Big(IL + VL(image\,background)\Big)\Big), \quad (1)$$

where L_{nu} is the luminance threshold for a nonuniform background (cd/m^2), L_u is the luminance threshold for the uniform dark background (cd/m^2), t is the adaptation time (s), *DICOM* is the DICOM standard display function (2011) resulting in the smallest detectable luminance difference (cd/m^2), *ALF* refers to adaptation luminance function (cd/m^2; Murdoch & Heynderickx, 2012), *IL* is the luminance of the image background (cd/m2), and *VL* is the veiling luminance (cd/m^2; Vos & van den Berg, 1999). Hence, the veiling luminance (VL) of the image background is computed and added to the image background luminance (IL).The ALF function then weights the image background luminance corrected for veiling luminance with the combination of Gaussians and integrates the outcome, calculating the adaptation luminance at the center of the target. Next, the DICOM function is used to calculate the smallest detectable luminance difference on the location of the center of the target (assumed to be in the fovea), for this adaptation luminance. Finally, this outcome is added linearly to the luminance threshold as a function of time for a uniform dark background.

Model performance

We tested the goodness of fit of this model to the data of Experiment E2. To do so, first, the black level visibility (the second term of Equation 1) was calculated for the three spatially nonuniform backgrounds of Experiment E2, using the model of Murdoch and Heynderickx (2012) as described above. The viewing position was assumed to be the location of the target. The output of this part of the model (the smallest detectable luminance difference for spatially nonuniform backgrounds) was then added linearly to the luminance threshold as a function of time for the spatially uniform background resulting from Experiment E1. The resulting sum of these values gave the predicted luminance threshold as a function of time for detecting a target in a nonuniform background. These predicted luminance thresholds were compared to the median of the measured adaptation time for every target's luminance level used in Experiment E2. Figure 10 shows the predicted luminance threshold (as a dashed line) and the target luminance levels (as dots) as a function of the corresponding median adaptation time for the three backgrounds used in Experiment E2 as a separate graph. The R^2 values of the model were 0.78, 0.85, and 0.88 for *Bar9*, *Bar2.7,* and *Square,* respectively. This shows that the prediction was reasonably good.

Although this relatively simple model is a good first approximation of the luminance threshold during dark adaptation for nonuniform backgrounds, there is still room for improvement. First, more variation in luminance distribution around the target and in (target) luminance levels may lead to a more accurate prediction of the luminance thresholds. Using more than two Gaussians in the adaptation luminance function may also improve the accuracy of the model. A good starting point would be to combine the model describing foveal sensitivity of Vangorp et al. (2015)

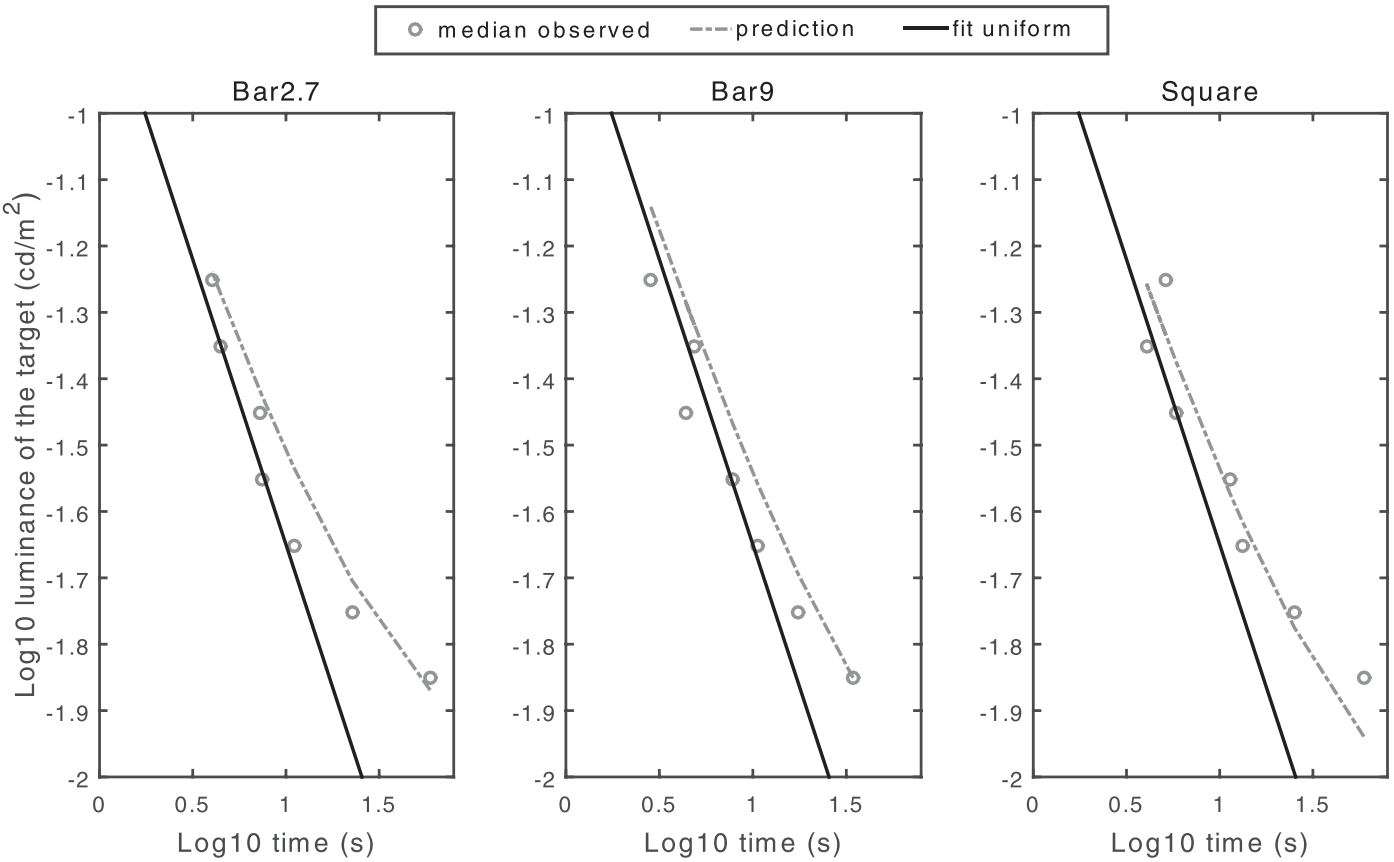

Figure 10. Graphical overview of the median adaptation times for every target luminance as measured in Experiment E2 (given by the dots), and the predicted luminance thresholds for those adaptation times (given by the dashed lines) for the nonuniform backgrounds *Bar9*, *Bar2.7*, and *Square*. The solid black line shows the fit of the luminance threshold as a function of time for the uniform background. Deviations from this solid line indicate the degree of local spatial adaptation for these backgrounds. The ^{10}log adaptation time (s) is presented on the *x*-axis and the ^{10}log adaptation luminance (cd/m^2) is presented on the *y*-axis.

with the model of Murdoch and Heynderickx (2012). However, Vangorp et al. (2015) only predict the adaptation state for the central part of the retina. Therefore, using our stimuli, which are varied in luminance distribution at larger visual angles, we cannot verify the potential improvement in accuracy of the combined models. Thus, more research is required to study the optimal combination of Gaussian functions describing foveal and peripheral sensitivity. Finally, as discussed before, the model may be extended by factors accounting for the movement of the viewing direction or for fluctuations in luminance levels in the background over time. Extending the model to take this into account provides a more realistic comparison to real life conditions.

General conclusion

In this study, dark adaptation was measured for three different spatial luminance distributions surrounding a to be detected target, while keeping the veiling luminance at the center of the target equivalent. The results prove that, for the nonuniform backgrounds used in the present study, the visual system adapts to a large extent to local luminance surrounding the viewing direction. Backgrounds with bright areas close to the viewing direction have longer adaptation times than backgrounds with bright areas positioned at a larger visual angle. In addition, any spatially nonuniform background results in a longer adaptation time compared to a spatially uniform dark background. This is the case even if the bright area is at an angle of 9° with respect to the target. This implies that also luminance values in the near periphery of the eye influence the adaptation process.

Based on the results, a simple model is proposed to predict the luminance threshold for a nonuniform background during dark adaptation. The model consists of the black level visibility model of Murdoch and Heynderickx (2012) in combination with a function describing the temporal change of the luminance threshold for adaptation to a uniform dark back-

ground. Results showed that the model predicts the observed data for spatially nonuniform backgrounds quite well. Still, extension of this model is needed to fully predict luminance thresholds during everyday activities, such as driving at night. Eventually such a model may lead to a better understanding of the visibility and even more important invisibility of objects encountered during, for example, nighttime.

Keywords: dark adaptation, veiling glare, local adaptation, spatial luminance distribution

Acknowledgments

The authors would like to thank Michael Murdoch, Dragan Sekulovski, and Lou Di for their valuable input in this study. This research was performed within the framework of the strategic joint research program on intelligent lighting between TU/e and Koninklijke Philips N.V.

Commercial relationships: Philips Research partly funded the project, and provided the lab facilities. Philips Research did not have any additional role in the study design, data collection and analysis, decision to publish, or preparation of the manuscript.
Corresponding author: Mariska Stokkermans.
Email: m.g.m.stokkermans@tue.nl.
Address: Eindhoven University of Technology, Eindhoven, The Netherlands.

References

Baker, H. D. (1953). The instantaneous threshold and early dark adaptation. *Journal of the Optical Society of America*, *43*, 798–803.

Baker, H. D. (1963). Initial stages of dark and light adaptation. *Journal of the Optical Society of America*, *53*, 98–103.

Crawford, B. H. (1947). Visual adaptation in relation to brief conditioning stimuli. *Proceedings of the Royal Society of London. Series B*, *134*, 283–302, http://doi.org/10.1098/rspb.1947.0015.

Daly, S., & Golestaneh, S. A. (2015). Use of a local cone model to predict essential CSF light adaptation behavior used in the design of luminance quantization nonlinearities. In B. E. Rogowitz, T. N. Pappas, & H. de Ridder (Eds.), *SPIE Proceedings: Vol. 9394. Human Vision and Electronic Imaging XX* (p. 939405). San Francisco, CA: SPIE. http://doi.org/10.1117/12.2083736.

Deeley, R. J., Drasdo, N., & Charman, W. N. (1991). A simple parametric model of the human ocular modulation transfer function. *Ophthalmic and Physiological Optics*, *11*, 91–93.

Digital Imaging and Communications in Medicine (DICOM). (2011). Grayscale standard display function. In *Digital imaging and communications in medicine* (pp. 1–55). Rosslyn, VA: National Electrical Manufacturers Association.

Eriksson, L. (2008). *Design of experiments: Principles and applications*. Umea, Sweden: MKS Umetrics AB.

Goffart, L., Quinet, J., Chavane, F., & Masson, G. (2006). Influence of background illumination on fixation and visually guided saccades in the rhesus monkey. *Vision Research*, *46*, 149–62. http://doi.org/10.1016/j.visres.2005.07.026.

Haig, C. (1941). The course of rod dark adaptation as influenced by the intensity and duration of pre-adaptation to light. *The Journal of General Physiology, 24*, 735–751.

Hecht, S., Haig, C., & Chase, A. M. (1937). The influence of light adaptation on subsequent dark adaptation of the eye. *The Journal of General Physiology, 20*, 831–850. Retrieved from http://jgp.rupress.org/content/20/6/831.abstract.

Hecht, S., Haig, C., & Wald, G. (1935). The dark adaptation of retinal fields of different size and location. *The Journal of General Physiology, 19*, 321–337.

Holladay, L. L. (1926). The fundamentals of glare and visibility. *Journal of the Optical Society of America*, *12*, 271–319.

Hood, D. C., & Finkelstein, M. A. (1986). Sensitivity to light. In K. Boff, L. Kaufman, & J. Thomas (Eds.), *Handbook of perception and visual performance, Volume 1: Sensory Processes and Perception* (pp. 5.1–5.66). New York, NY: John Wiley & Sons.

Langendijk, E. H. A., & Hammer, M. (2010). 14.4: Contrast requirements for OLEDs and LCDs based on human eye glare. In *Society of Information Display* (pp. 192–194). Oxford, UK: Blackwell Publishing Ltd.

Lankheet, M. J. M., Przybyszewski, A. W., & van de Grind, W. A. (1993). The lateral spread of light adaptation in cat horizontal cell response. *Vision Research*, *33*, 1173–1184.

Lee, B. B., Dacey, D. M., Smith, V. C., & Pokorny, J. (1999). Horizontal cells reveal cone type-specific adaptation in primate retina. *Proceedings of the National Academy of Sciences, USA*, *96*, 14611–14616. http://doi.org/10.1073/pnas.96.25.14611.

Miller, S., Nezamabadi, M., & Daly, S. (2012). Perceptual signal coding for more efficient usage of bit codes. In *SMPTE annual technical conference exhibition* (pp. 52–59). White Plains, NY: SMPTE.

Moon, P., & Spencer, D. E. (1945). The visual effect of non-uniform surrounds. *Journal of the Optical Society of America*, *35*, 233–247.

Mote, F. A., & Riopelle, A. J. (1951). The effect of varying intensity and the duration of pre-exposure upon foveal dark adaptation. *The Journal of General Physiology*, *34*, 657–674.

Murdoch, M. J., & Heynderickx, I. (2012). Veiling glare and perceived black in high dynamic range displays. *Journal of the Optical Society of America*, *29*, 559–566.

Normann, R. A., Baxter, B. S., Ravindra, H., & Anderton, P. J. (1983). Photoreceptor contributions to contrast sensitivity: Applications in radiological diagnosis. *IEEE Transactions on Systems, Man, and Cybernetics, 13*(5), 944–953.

Osborne, J. W., & Overbay, A. (2004). The power of outliers (and why researchers should always check for them). *Practical Assessment, Research & Evaluation*, *9*, 1–12.

Pokorny, J., & Smith, V. (1997). Psychophysical signatures associated with magnocellular and parvocellular pathway contrast gain. *Journal of the Optical Society of America A*. *15*, 2440–2442. http://doi.org/10.1364/JOSAA.15.002440.

Ruseckaite, R., Lamb, T. D., Pianta, M. J., & Cameron, A. M. (2011). Human scotopic dark adaptation: Comparison of recoveries of psychophysical threshold and ERG b-wave sensitivity. *Journal of Vision*, *11*(8):2, 1–16, doi:10.1167/11.8.2. [PubMed] [Article]

Rushton, W. A. H., & Westheimer, G. (1962). The effect upon the rod threshold of bleaching neighbouring rods. *Journal of Physiology*, *164*, 318–329.

Snodderly, D. M. (1987). Effects of light and dark environments on macaque and human fixational eye movements. *Vision Research*, *27*, 401–415. http://doi.org/10.1016/0042-6989(87)90089-7.

Stokkermans, M. G. M., & Heynderickx, I. E. J. (2014). Temporal dark adaptation to spatially complex backgrounds: Effect of an additional light source. *Journal of the Optical Society of America*, *31*, 1485–1494.

Uchida, T., & Ohno, Y. (2013). Defining the visual adaptation field for mesopic photometry: Does surrounding luminance affect peripheral adaptation? *Lighting Research and Technology*, *46*(5), 520–533. Retrieved from http://lrt.sagepub.com/cgi/doi/10.1177/1477153513498084.

Vangorp, P., Myszkowski, K., Graf, E. W., & Mantiuk, R. K. (2015). A model of local adaptation. *ACM Transactions on Graphics, 34*(6), 166:1–166:13.

Vos, J. J. (2003). Reflections on glare. *Lighting Research and Technology*, *35*, 163–176. http://doi.org/10.1191/1477153503li083oa.

Vos, J. J., & van den Berg, T. J. T. P. (1999). Research note: Disability glare. *Vision and Colour: Physical Measurement of Light and Radiation, CIE Collection, No. 135,* 1–78.

Wald, G., & Clark, A. (1937). Visual adaptation and the chemistry of the rods. *The Journal of General Physiology*, *21*, 93–105.